Drying of polymer powder in fluidized bed. Modelling of multizone dryer

Nickolay M. Ostrovskii

Hipol a.d., Odžaci, Serbia

Abstract

The process of drying of porous polymer powder (polypropylene) intended to remove the solvent (heptane) is analyzed. The dryer consists of two stages (apparatus) with multizone fluidized bed. The mathematical model of the process in multizone fluidized bed is proposed. The rate-limiting step, depending on diameter of polymer particles, is determined. It was found that in relatively large particles (>200 μm) the rate of drying is limited by intraparticle diffusion. A way to decrease the energy consumption in drying has been also discussed and verified in experiments.

Keywords: polymer powder drying, fluidized bed, rate limiting step, multizone dryer, mathematical model.

Available online at the Journal website: http://www.ache.org.rs/HI/

Polymers

SCIENTIFIC PAPER

UDC 676.742.3:66.047:51

Hem. Ind. **68** (6) 661–671 (2014)

doi: 10.2298/HEMIND131016007O

Many polymerization processes are carried out in suspension, which consists of liquid monomer itself (or its solution in some solvent) and of growing polymer particles. At the reactor exit, porous polymer particles should separate from the suspension. If the liquid is not ease vaporable, then first centrifugation and next drying stages are used for separation. An example of such a process is the propylene polymerization over solid Ziegler–Natta catalysts in heptane or hexane solution. After centrifugation, the polymer powder (50––500 μm) contains 15–20% of heptane in its pores.

For such a powder (as well as for corns, inorganic and pharmaceutical materials) the fluidized-bed drying is widely used. It provides a good mixing of powder, easy heat application, a relatively homogeneous temperature and a continuous process operation (Fig. 1).

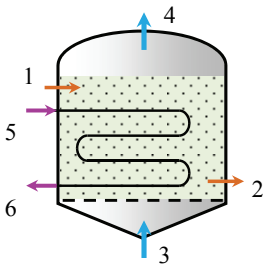

Figure 1. Schematic diagram of fluidized-bed dryer. 1, 2 – particles flow; 3, 4 – gas flow; 5, 6 – heat-transfer flow.

Most of the gas passes through the fluidized bed in the form of bubbles, which almost do not contain solids. Bubbles merge and disintegrate in the bed, and collapse at the exit of bed. Thus, the fluid provides almost ideal mixing of solids, and prevents from local overcooling and particles agglomeration.

On the other hand, bubbles diameter (3–10 cm) considerably exceeds the typical particles diameter (0.02–1 mm). This reduces the interface area (gas––particles) that becomes equal to the external surface of bubbles, and consequently, slows down the rate of mass transfer (rate of drying).

Therefore, the bubble fragmentation in fluidized bed is desirable. It is possible in so-called “organized fluidized bed” with small-volume packing, grates, or even with immersed heaters (like in Fig. 1).

The size of polymer particles varies from 20 to 550 μm. The particles size distribution, coupled with the mixing of solid phase, generates the distribution of particles residence time in a fluidized bed. That is why at the exit of bed, there is always a mixture containing particles from “almost dry” to “almost wet”. The distribution of particles moisture determines the average polymer moisture that should satisfy the requirements of polymer quality (0.1%).

The mathematical model of drying process should include all peculiarities (mentioned above) if the purpose of modelling is a detail analysis and optimization. Heat balance equations should enclose a fluid convection, an interphase heat transfer, and a mixing of solid phase. Mass balance equations (for both fluid and solid moisture) also should represent phase flow velocities, an interphase mass transfer, and a moisture transfer inside particles.

Such a model is constructed in present paper and is applied to the drying of polypropylene powder in multistage dryer with fluidized bed. For the solid phase moisture and temperature the model of “exchange interaction“ between zones is used. The rate limiting step is examined, depending on particles size and moisture. The energy efficiency is also analysed in order to decrease the heat consumption.

Correspondence: Hipol a.d., Gračački put b.b., 25250 Odžaci, Serbia Serbia.

E-mail: nikolaj.ostrovski@hipol.rs

Paper received: 16 October, 2013

Paper accepted: 7 February, 2014

Total heat balance of the process

Let us consider the structure of energy consumption in a drying process. The heat is consumed for the heating of polymer powder, heptane and nitrogen to the drying temperature, as well as for heptane evaporation:

$$\left(G_{LPS}+G_{MPS}\right)Q_W = G_S\left(Cp_S+\frac{G_H}{G_S}Cp_H\right)\left(T_S-T_S^o\right)+ \\ +F_G\,Cp_G\,\rho_G\left(T_G-T_G^o\right)+G_H\,Q_H \tag{1}$$

Specific consumption of water steam depends on input moisture of polymer powder (heptane concentration), $W_o = G_H/(G_S + G_H)$:

$$\frac{G_{LPS}+G_{MPS}}{G_S}=\frac{1}{Q_W}\left(Cp_S+\frac{W_o}{1-W_o}Cp_H\right)\left(T_S-T_S^o\right)+ \\ +\frac{F_G\,\rho_G}{G_S}\frac{Cp_G}{Q_W}\left(T_G-T_G^o\right)+\frac{W_o}{1-W_o}\frac{Q_H}{Q_W} \tag{2}$$

The Eq. (2) is illustrated in Fig. 2. It is seen that the total consumption of steam is much higher than required for heptane evaporation. It means that probably some potential opportunities exist for the saving of heat energy. For example, almost half water steam is supplied for a heating of nitrogen. Its mass flow ($F_G\rho_G$) depends on dryer capacity and optimal fluidization velocity, and therefore cannot be decreased. Meanwhile, the contribution of nitrogen in total heat balance of the process is quite low (less than 12%), because of low heat capacity (Cp_G) and low difference of temperatures ($T_G - T_S$).

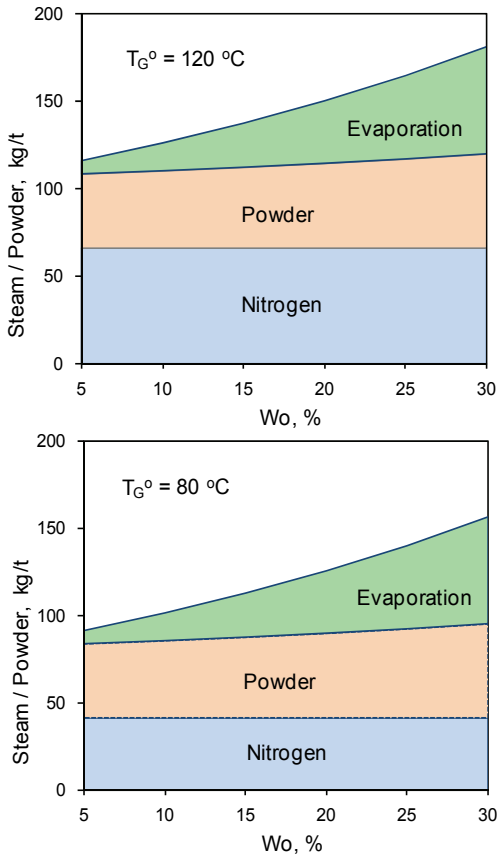

Figure 2. Specific consumption of water steam for the polymer drying as a function of input moisture of powder. (Hipol a.d., 2007).

Thus, the temperature of input nitrogen (T_G^o) can be optimized in order to decrease the energy consumption (Fig. 2). Besides, when the temperature T_G^o is decreased from 120 to 80 °C, the middle-pressure steam (MPS, 11 bar) can be replaced by low-pressure steam (LPS, 2 bar).

Nevertheless, a decreasing of T_G^o can cause some undesirable changes in drying dynamics, which is impossible to estimate on the base of only total heat balance. For this purpose, a detail modelling of dryer is necessary based on drying kinetics (Eqs. (11)–(17)), equations of mass and heat balance (Eqs. (18)–(26)), and fluidized bed hydrodynamics (Eqs. (27)–(30)).

Process in particle

For the description of heptane concentration inside particle (moisture of particle, w_r) the diffusion equation can be used [1–3]:

$$\frac{\partial w_r}{\partial t}=D_P\left(\frac{\partial^2 w_r}{\partial r^2}+\frac{s}{r}\frac{\partial w_r}{\partial r}\right) \tag{3}$$

It not represents the actual mechanism of moisture transfer in porous particles, which is the combination of diffusion, capillary and surface phenomena [3]. Nevertheless, it gives the possibility to estimate the rate of particles drying or corresponding time.

At the particle center the symmetry condition is valid:

$$r = 0:\ \mathrm{d}w_r/\mathrm{d}r = 0 \tag{4}$$

At the external particle surface, the diffusion flux from the particle is equal to the rate of mass transfer through the external laminar layer of fluid:

$$r = R_P:\ D_P\frac{S_P}{V_P}\frac{d\,w_r}{d\,r}=\frac{k_m}{\rho_P}\frac{S_P}{V_P}\left(C-C_E\right) \tag{5}$$

Defining the dimensionless radius, $\phi = r/R_P$, we obtain:

$$\phi = 1:\ \frac{\mathrm{d}w_r}{\mathrm{d}\phi}=\frac{\mathrm{Bi}}{\rho_P}\left(C-C_E\right),\ \mathrm{Bi}=\frac{k_m R_P}{D_P} \tag{6}$$

The mass transfer Biot number (Bi) indicates the ratio of external mass transfer and internal diffusion. Let's try to estimate the value of Bi. An effective dif-

fusivity in porous particle depends on its moisture $\psi(w)$, porosity (ε_P), and porous tortuosity (h):

$$D_P(w) = \psi(w) D_m \varepsilon_P / h \quad (7)$$

Molecular diffusivity in gas phase (heptane in nitrogen) consist of D_{mG}, from 7×10^{-2} to 9×10^{-2} cm^2/s, and in liquid phase D_{mL}, from 3×10^{-5} to 8×10^{-5} cm^2/s [4]. The particle porosity varies in the range 0.15–0.25 and the tortuosity, h, in range 4–6 [5].

The most complicated is ψ parameter, which represents an influence of surface tension and osmotic and capillary effects [3]. It decreases with w and vary in the interval 0.02–0.1.

The mass transfer coefficient, k_m, is usually changed within 10–100 cm/s [6]. Then, Biot number values reach 10^2–10^3 (in the case of gas phase diffusion) and 10^5–10^6 (liquid phase diffusion).

Because of Bi >> 1, the rate of external mass transfer is always higher than the rate of internal diffusion, which is therefore the rate limiting step of the process.

In the case of small particles (<1 mm), it is not necessary to calculate the moisture distribution inside particles, and it is sufficient to estimate the integral (average) moisture:

$$W = \int_0^{R_P} 3\frac{r^2}{R_P^3} w_r(r)\,dr \quad (8)$$

Because of Bi >>1, at the particle surface ($r = R_P$) we have $w_r(R_P) = W_E$. Thus, after integrating Eqs. (3) and (8) we obtain the well-known approximate solution:

$$w = \frac{W - W_E}{W_o - W_E} \approx \frac{6}{\pi^2} \exp\left(-\pi^2 \frac{D_P}{R_P^2} t\right) \quad (9)$$

The example of drying dynamics of polymer particles, according to Eq. (9), is presented in Fig. 3a. Drying time is proportional to particle diameter as square. For example, in the case of d_P = 50 μm, the moisture reducing from 16 to 1.6 %, requires the only 0.2 min. Meanwhile, for particles having diameter d_P = 350 μm, this time is increased up to 12 min.

In a fluidized bed (even with uniform particles), the non-uniform distribution of residence time $f(t)$ exists (Fig. 4), which is tended to a normal distribution with increasing of n [2]:

$$f(t) = \frac{1}{\tau_Z (n-1)!} \left(\frac{t}{\tau_Z}\right)^{n-1} \exp\left(-\frac{t}{\tau_Z}\right)$$

That is why the average moisture, $\langle w \rangle$, differs from the moisture estimated by Eq. (9). For the bed having only one stage, the Eq. (10) can be used for $\langle w \rangle$ calculation (Fig. 3b):

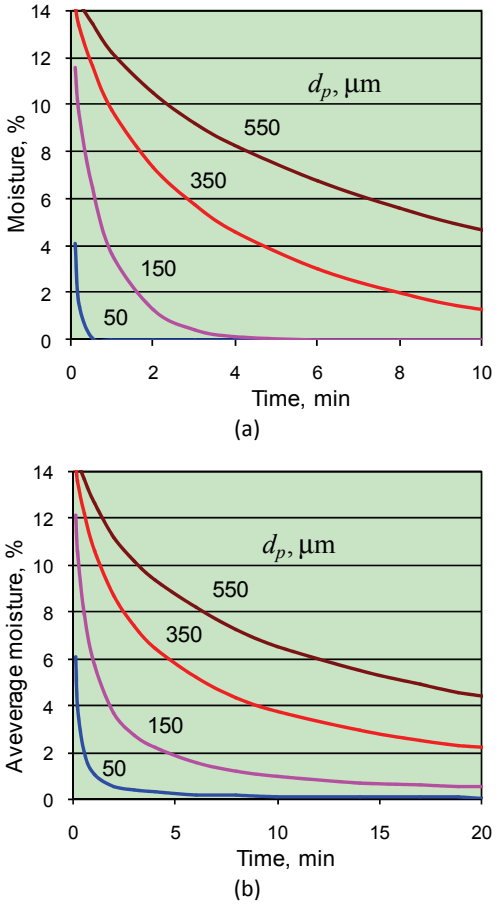

Figure 3.a) Particle drying dynamics in accordance with Eq. (9) and b) particle drying dynamics in fluidized bed in accordance with Eq. (10); W_O = 16%, W_E = 0.1%; $D_P = 1\cdot10^{-7}$ cm^2/s.

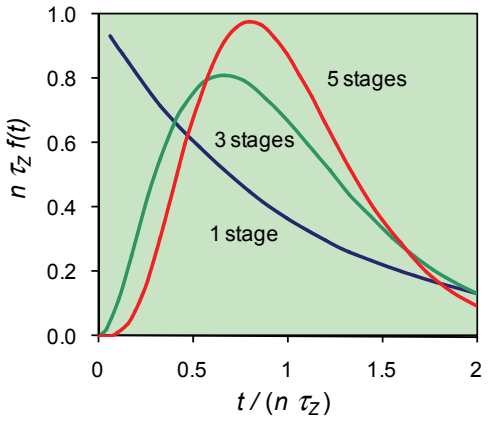

Figure 4. Distribution function of particles residence time in multi-stage (n) fluidized bed.

$$\langle w \rangle = \frac{1}{\tau_Z} \int_0^{\infty} \exp(-t/\tau_Z)\, w(t)\, dt \approx \approx \frac{6}{\pi^2} \left(1 + \pi^2 \frac{D_P}{R_P^2} \tau_Z\right)^{-1} \quad (10)$$

From the comparison of Fig. 3a and b, it is seen that the drying time in fluidized bed (under particles mixing) is two times longer than without mixing. Such an influence of residence time distribution should be taken into account during analysis of fluidized bed dryer.

Mass transfer in fluidized bed

Another peculiarity of fluidized bed is the influence of external mass transfer. The rate of gas-solid mass transfer in fluidized bed is lower than in the case of single freely settling particle. The reason is a bubbling regime of gas flow (about 90 %) passing through the suspension phase (Fig. 5). In this case the bubbles external surface determines the rate of mass transfer.

In any *j*-th zone of the bed (having volume V_j) the rate of mass transfer is given by

$$R_m = \beta_T V_j \frac{\rho_F}{\varepsilon_F}\left(W_j - W_E\right),\ W_E = H\,C_E \qquad (11)$$

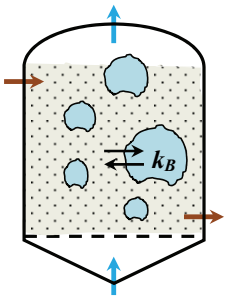

Figure 5. Interphase mass transfer in fluidized bed.

The value of total coefficient, β_T, depends on local coefficients:

1) β_P – inside particle to its surface, S_P:

$$\beta_P = k_P(S_P/V_P)(1-\varepsilon_F) = k_P(6/d_P)(1-\varepsilon_F) \qquad (12)$$

2) β_B – into bubble through its surface, S_B:

$$\beta_B = k_B(S_B/V_B)\varepsilon_F = k_B(6/d_B)\varepsilon_F \qquad (13)$$

Here $(S_B/V_B)\varepsilon_F = a_B$ and $(S_P/V_P)(1-\varepsilon_F) = a_P$ are specific areas of bubbles and particles in the unit of bed volume (cm^2_i/cm^3_{bed}). So, the coefficients β_P, β_B, and also β_T, have the same unit ($cm^3_{gas}/(cm^3_{bed}$ s)). Because of successive steps (12) and (13), their rates are equal each other in quasi-steady state and equals to R_m. Then, the total coefficient, β_T, is defined by formula:

$$\frac{1}{\beta_T} = \frac{1}{\beta_P} + \frac{1}{\beta_B} \qquad (14)$$

The local transfer coefficient in bubble (k_B, $cm^3_{gas}/(cm^2_{bubble}$ s)) depends on hydrodynamic regime in fluidized bed, namely on bubble diameter (d_B) and on its velocity (u_B), which is indirectly dependent on particles diameter (d_P) [2]:

$$k_B = \left(\frac{d_B^{5/4}}{a + b d_B^{1/4}} + \frac{d_B^{3/2}}{c u_B^{1/2}}\right)^{-1} \qquad (15)$$

a, *b* and *c* are empirical parameters.

The local transfer coefficient in particle (k_P, $cm^3_{gas}/(cm^2_{particle}$ s)) approximates the diffusion flux inside particle, similarly to first member of Eq. (5):

$$k_P a_P \left(W - W_E\right) \approx \varepsilon_P \frac{D_P}{R_P}\frac{\rho_L}{\rho_G} a_P \frac{\mathrm{d}W}{\mathrm{d}\phi} \qquad (16)$$

Then k_P can be defined by formula:

$$k_P = \frac{2 D_P \varepsilon_P}{d_P\,\Delta\phi}\frac{\rho_L}{\rho_G},\ \Delta\phi = 1 - \delta_o\left(W/W_o\right)^{1/3} \qquad (17)$$

The parameter $\Delta\phi$ is a formal dimensionless depth of a dry zone in particle, through which the moisture is diffused. It is increased from $1-\delta_o$ at the beginning, when $W = W_O$, to ~1 at the end of the process, when $W \approx W_E$. Thus, the coefficient k_P (or D_P) is decreased in drying process, which is typical for capillary-porous materials [3].

Anticipated values of parameters β_B and β_P are presented in Fig. 6. They were calculated using formulas (12)–(17) under conditions of drying of polypropylene powder.

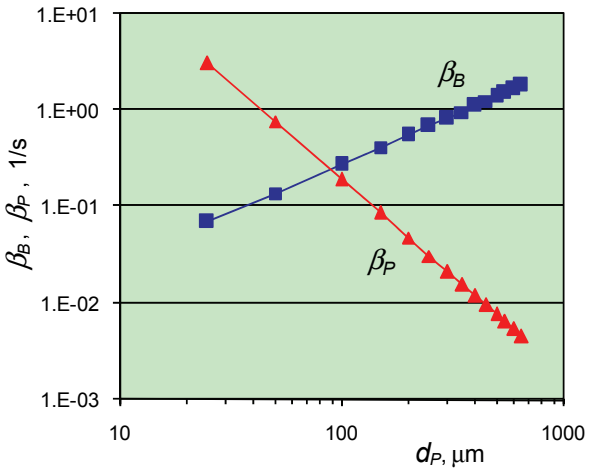

Figure 6. Dependencies of mass-transfer coefficients on particle diameter.

In contrast to mass transfer under the blowing of a single particle, there is a little difference between the intensity of external (through bubble surface) and internal (through particle surface) mass transfer here (Fig. 6).

In the case of relatively large particles (>200 μm), $\beta_P < \beta_B$, therefore the rate of process is limiting by moisture diffusion in particles, and $\beta_T \approx \beta_P$. In the case of fine particles (<50 μm), $\beta_B < \beta_P$, therefore the rate of process is limiting by mass transfer in bubbles, and

$\beta_T \approx \beta_B$. In transition region (50–200 μm), the formula (14) should be used.

In polymerization process, the polydisperse particles are usually formed, and their size distribution depends on the catalyst type (Fig. 7). That is why particles separation along the height of fluidized bed always takes place. Consequently, the distribution of particles residence time in a dryer becomes rather complicated. These are the main reasons of application of multi-stage fluidized bed dryer in industry.

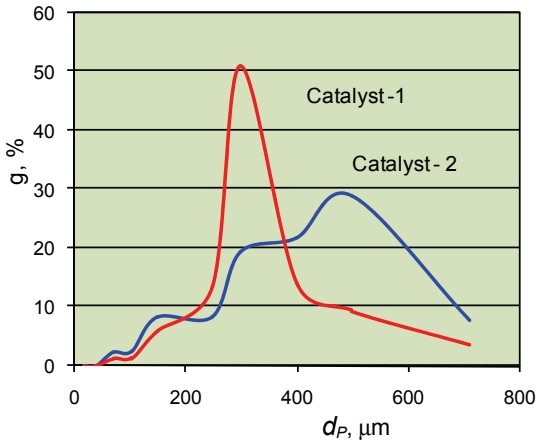

Figure 7. The distribution of polypropylene particles size depending on polymerization catalyst; initial moisture W_O (% of heptane): catalyst 1: 16–18%; catalyst 2: 17–25%.

Zones of fluidization in dryer

The simplified scheme of drying of polypropylene powder (PP) is presented in Fig. 8. Each stage of dryer is divided in two parts by vertical curtain wall. The powder is transferred from the left part to the right part under this wall. The heat is supplied in dryers by two ways: 1 – by heating of fluidized bed using water low-pressure steam (LPS, 2 bar), supplying in heat radiators; 2 – by heating of fluid (N_2) in heat exchangers using water middle-pressure steam (MPS, 11 bar).

Because of these peculiarities of dryer design (Nara Machinery, Japan), the hydrodynamic regime in process vessels is quite complicated (Fig. 9). Each fluidization vessel can be divided in three groups of zones distinguished by hydrodynamic conditions. Upper zones (1, 6 and 7, 12) are located over radiators. Middle zones (2, 5 and 8, 11) occupy the majority of a bed volume, where radiators are allocated. Lower zones (3, 4 and 9, 10) represent the space between radiators and gas distributors (perforated metal grates).

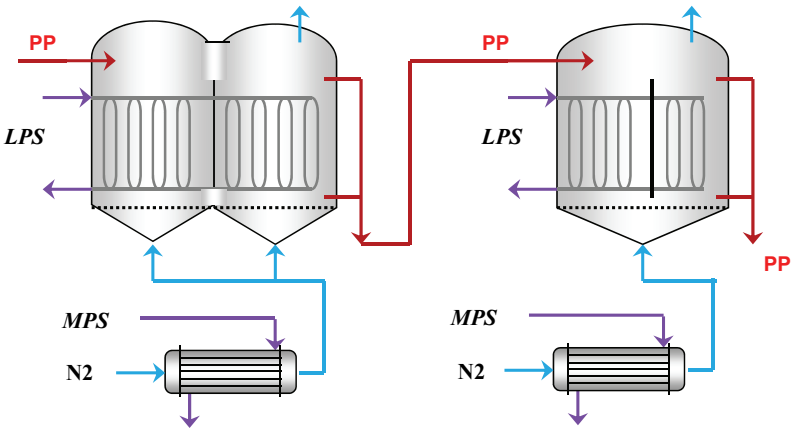

Figure 8. The principle circuit of PP drying.

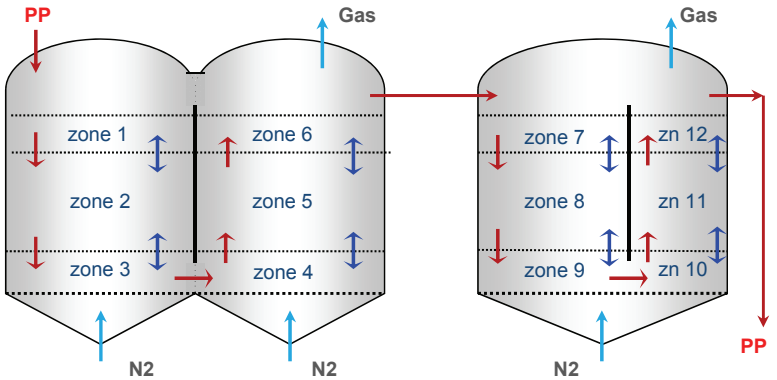

Figure 9. Solids flow scheme in dryers; ↓ – flow; ↕ – mixing.

Mathematical model of the process

Each mentioned zone we can consider to be completely mixed stage, which is typical for a fluidized bed [2,6]. For the drying process modelling, four equations are necessary in each zone. They are: moisture concentrations in gas and solid phases, as well as gas and solid temperatures. Thus, for dryer with 12 zones, this implies a model with 48 equations. Besides, heat balance equations in radiators and in heat exchangers should be formulated.

Gas phase (bubbles)

The moisture concentration in gas (C) and the gas temperature (T_G) are changed due to the gas streaming and interphase transfer:

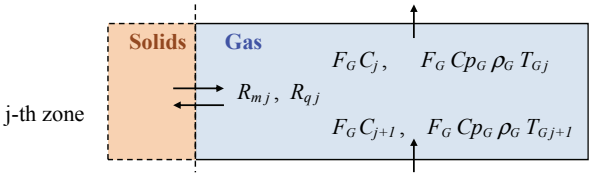

Rates of mass and heat transfer:

$$R_{mj} = \beta_T V_j \frac{\rho_F}{\varepsilon_F}\left(W_j - W_E\right),\ R_{qj} = \alpha_T V_j \left(T_{Gj} - T_{Sj}\right) \tag{18}$$

Balance equations:

$$F_G\left(C_j - C_{j+1}\right) = R_{mj}\ ,\ F_G Cp_G \rho_G \left(T_{Gj} - T_{Gj+1}\right) = R_{qj} \tag{19}$$

Dense phase (particles)

The process in a dense phase is much more complicated. Except the main flow of solids (input-output, G_S), the interstage particles transfer takes place. This transfer is the result of fluidization and is interpreted often as particles diffusion (axial dispersion). Such a flux provides an interchange of moisture and heat between zones. Thus, corresponding rate coefficients of these mass (D_S) and heat (λ_S) transfer can be defined by formula:

$$D_{Sj} = D_F \frac{F_j}{L_j}\rho_F\ \left(1-\varepsilon_F\right),\ \lambda_{Sj} = \lambda_F \frac{F_j}{L_j} \tag{20}$$

In a heat balance, a significant role plays the heating of solids by immersed radiator (R_R) and the cooling by heptane evaporation (Q_H). The rate of heating is proportional to the difference of temperature in zones 2, 5, 8 and 11, and in radiators:

$$R_{Rj} = \alpha_R V_j \left(T_{Rj} - T_{Sj}\right) \tag{21}$$

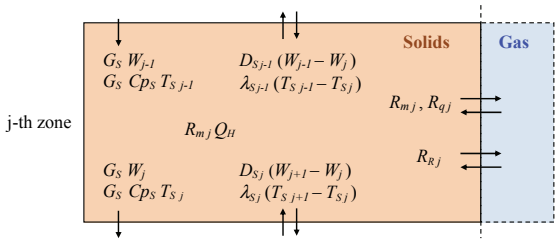

Mass and heat balance equations in a j-th zone:

$$G_S\left(W_j - W_{j-1}\right) = D_{Sj}\left(W_{j+1} - W_j\right) + \\ + D_{Sj-1}\left(W_{j-1} - W_j\right) - R_{mj} \tag{22}$$

$$Cp_S G_S\left(T_{Sj} - T_{Sj-1}\right) = \lambda_{Sj}\left(T_{Sj+1} - T_{Sj}\right) + \\ + \lambda_{Sj-1}\left(T_{Sj-1} - T_{Sj}\right) + R_{qj} + R_{Rj} + R_{mj} Q_H \tag{23}$$

Heating

Heat balance equation in a radiator:

$$G_{LPSj} Cp_{LPS}\left(T_{LPS} - T_{Rj}\right) + G_{LPSj} Q_W = R_{Rj} \tag{24}$$

Balance equation in a heat exchanger (for the heating of N_2):

$$F_G Cp_G \rho_G\left(T_G - T_G^o\right) = \\ = G_{MPS} Cp_{MPS}\left(T_{MPS} - T_G\right) + G_{MPS} Q_W \tag{25}$$

Overall heat balance in a fluidized bed:

$$Cp_S\left(G_S T_S - G_S^o T_S^o\right) + \left(G_S^o - G_S\right) Q_H = \\ = F_G Cp_G \rho_G\left(T_G^o - T_G\right) + G_{LPS} Q_W \tag{26}$$

Fluidization parameters

Most hydrodynamic characteristics of fluidized bed depend on Archimedes and Reynolds numbers:

$$\mathrm{Ar} = \frac{g d_P^3 \rho_P \rho_G}{\mu_G^2}\ ,\ \mathrm{Re}_P = \frac{u_G d_P \rho_G}{\mu_G} \tag{27}$$

Particular Reynolds numbers: current (Re_P), start of fluidization (Re_{PF}), and start of particle transport (Re_{PT}) are functions of Archimedes number. They give the possibility to calculate corresponding gas velocities [7]:

$$\mathrm{Re}_P = \frac{\mathrm{Ar}}{18 + 5.22\ \mathrm{Ar}^{0.5}},\ \mathrm{Re}_{PF} = \frac{\mathrm{Ar}}{1400 + 5.22\ \mathrm{Ar}^{0.5}}, \\ \mathrm{Re}_{PT} = \frac{\mathrm{Ar}}{18 + 0.61\ \mathrm{Ar}^{0.5}} \tag{28}$$

For the calculation of heat transfer coefficients (h_q, h_R) the Nusselt number is used [7]:

$$\mathrm{Nu}_q = \frac{h_q d_P}{\lambda_G} = 0.4\left(\frac{\mathrm{Re}}{\varepsilon_F}\right)^{2/3} \mathrm{Pr}^{1/3},$$

$$\mathrm{Nu}_R = \frac{h_R d_P}{\lambda_G} = 0.75\left(1 - \frac{d_c}{L_c}\right)^{0.14} \mathrm{Ar}^{0.22} \qquad (29)$$

In a fluidized bed hydrodynamics a bed porosity (ε_F), particles „diffusivity“ (D_F), and an effective heat conductivity of the bed (λ_F) are also very important [2]:

$$\varepsilon_F = \left(\frac{18\mathrm{Re} + 0.36\mathrm{Re}^2}{\mathrm{Ar}}\right)^{0.21}, \quad D_F = \frac{\alpha^2 d_B}{3\delta}\frac{\varepsilon_F}{u_F}\left(u_G - u_F\right)^2,$$

$$\lambda_F = D_F C p_S \rho_F \qquad (30)$$

Here α and δ are empirical functions of bubbles diameter.

The model should also include well-known equations for heat transfer coefficient in heat exchangers; for physical properties of nitrogen, heptane, water steam and polymer powder; for pressure drop in fluidized bed, etc. [4,6].

Modelling of drying process

First, the modelling of standard drying regime has been done (Fig. 10). It provides a drying of PP powder (3.8–4.1 t/h) from initial moisture of 15–18% to final moisture less than 0.1%. The temperature in 1st and 5th zone, and powder moisture at the exit of dryers are in a good agreement with experimental data (Fig. 10). From this simulation of drying process the following parameters were estimated: D_P , from 2.5×10^{-7} to 3.0×10^{-7} cm^2/s; D_F, 80–120 cm^2/s; d_B, 5–7 cm. The rest of parameters were calculated using the above formulas.

The bubbles diameter (d_B) is determined by distance between tubes of immersed steam radiator [8,9]. The axial dispersion of particles (D_F), calculated by (30), is also corresponded to latter estimations [10]. Finely, the effective intra-particle diffusivity (D_P) lies in the interval of values predicted by formula (7) at D_{mL} = 6.6×10^{-5} cm^2/s, ε_P = 0.2, h = 5, and ψ = 0.1.

Using these parameters, two regimes of drying process were simulated: 1st – at the N_2 inlet temperature T_G^o = 120 °C, and 2nd – at T_G^o = 80 °C. The results are presented in Fig. 11.

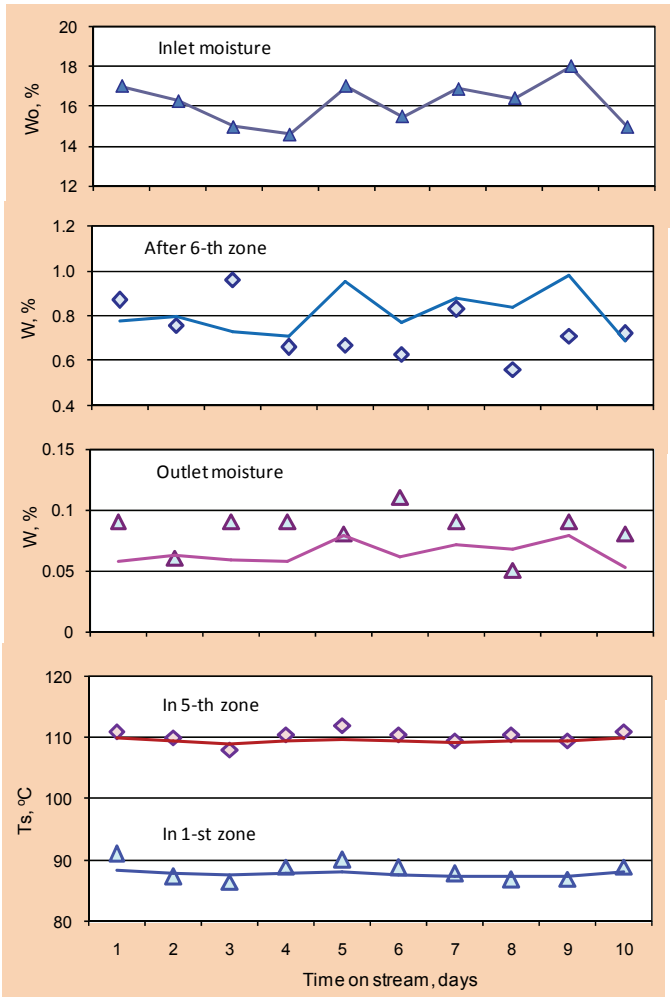

Figure 10. Results of standard regime modelling. G_S = 3.8-4.1 t/h, T_G^o = 120 °C. Points – experimental data; Lines – calculated values.

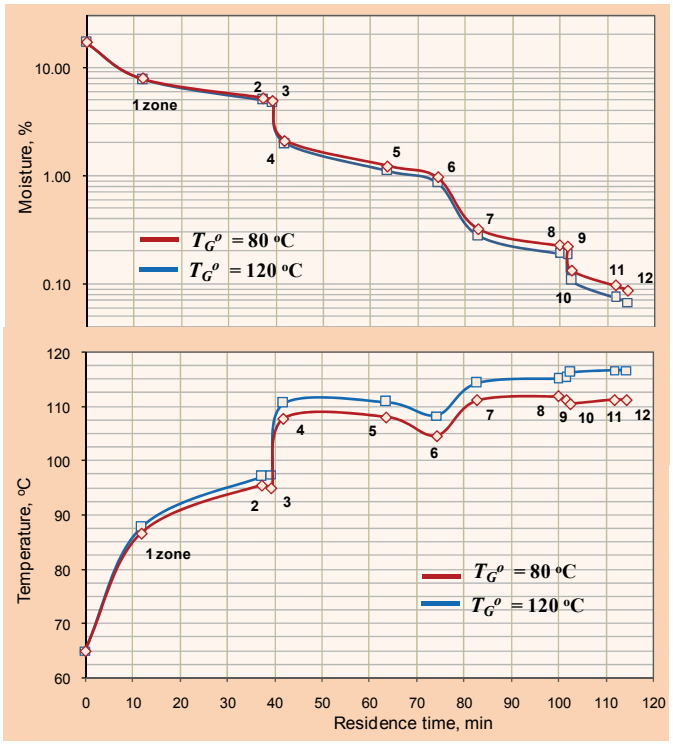

Figure 11. Results of dryer modeling: the influence of T_G^o. G_S = 3.94 t/h. Numbers indicate a zone number.

It is seen from Fig. 11 that supposed decrease in energy consumption, which has been made in Section „Total heat balance of the process“ and Fig. 2, is quite possible. The decreasing of T_G^o only slightly increases the outlet powder moisture, which remains lower than 0.1%.

Nitrogen mass flows, as well as flow rates of low-pressure steam (LPS) and middle-pressure steam (MPS) for these two regimes, are presented in Figs. 12 and 13. It is seen, that the decreasing of MPS by 130 kg/h increases the consumption of LPS by 110 kg/h without remarkable changing in zone temperature, and without loss of drying quality. It happens because the gas moisture (heptane content in N_2) affects the rate of drying much stronger than the gas temperature.

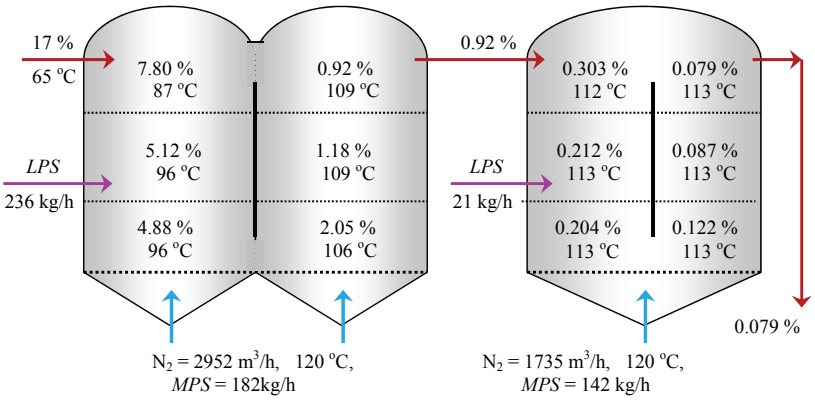

Figure 12. Results of standard regime modelling. G_S = 3.94 t/h of dry powder. T_G^o = 120 °C. Numbers – powder moisture and temperature in zones.

For the experimental verification of these regimes (and for the model validation), the trial run of dryer was carried out, and the results are presented in Fig. 14. The nitrogen inlet temperature T_G^o has been varied from 120 to 95 °C, and the inlet moisture of polymer – from 15 to 25%. It is clearly seen from Fig. 14 that the average outlet moisture is in acceptable correlation with the average inlet moisture at all nitrogen temperatures. The best illustration for the possibility of T_G^o decreasing is an operation at 95 and 120 °C at approximately the same inlet moisture of 22% (see interval from 95th to 170th days). Both cases (95 and 120 °C)

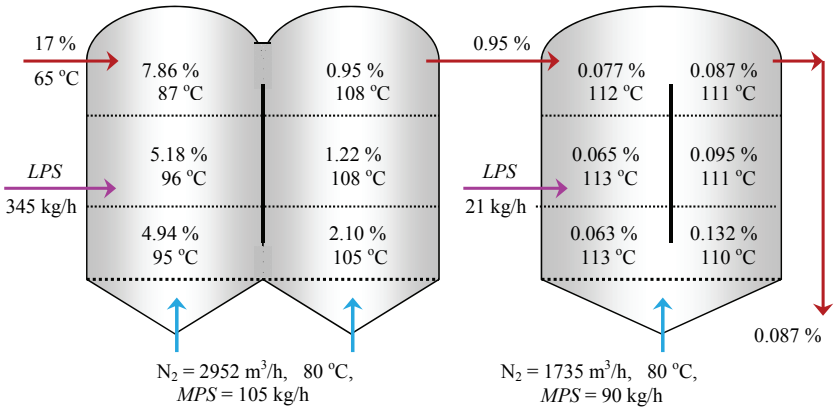

Figure 13. Results of modified regime modelling. G_S = 3.94 t/h of dry powder. T_G^o = 80 °C. Numbers – powder moisture and temperature in zones.

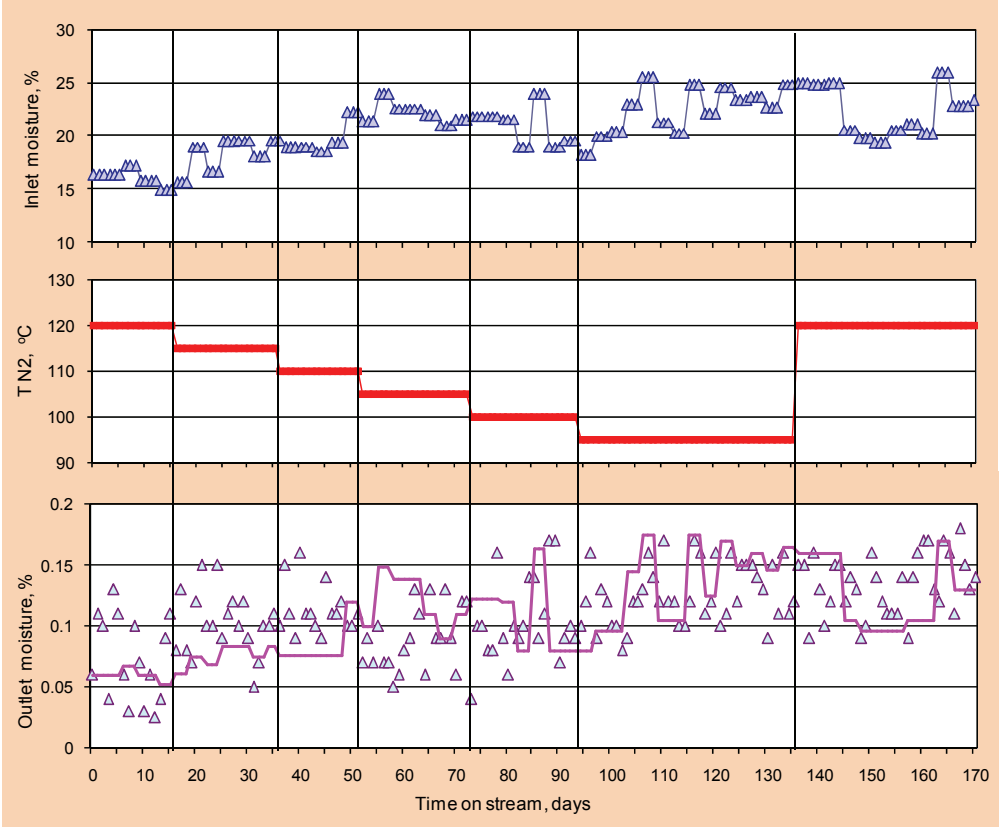

Figure 14. Trial run of dryer. G_S = 3.9–4.0 t/h of dry powder. T_G^o = 95-120 °C. Points – experimental values. Lines – calculated outlet moisture.

provide almost the same average outlet moisture of 0.12–0.13%.

These experiments open up the possibility to replace the middle-pressure steam (MPS) by low-pressure steam (LPS) for the heating of nitrogen.

CONCLUSIONS

The simulation based on the Multizone Model showed good agreement with experimental data. It was demonstrated that proposed model could also predict hydrodynamic and thermal behavior of multizone fluidized bed dryer with immersed heating tubes.

The model consists of plausible values of mass and heat transfer parameters.

The application of presented model is proved to be fruitful in optimization of dryer operation and of energy consumption.

Nomenclature

a_B, a_P specific area of bubble and particle [cm^2/cm^3 or m^2/m^3]

a_R specific area of radiator [m^2/m^3]
C, C_E current and equilibrium moisture content in gas [g/cm^3 or kg/m^3]
Cp_G, Cp_L, Cp_S heat capacity of gas, liquid and solid [J/(g K) or kJ/(kg K)]
Cp_{LPS}, Cp_{MPS} heat capacity of water steam [kJ/kg K]
d_B, d_P bubbles and particles diameter [cm]
d_c diameter of radiator pipe [cm]
D_m molecular diffusivity [cm^2/s]
D_P effective diffusivity in particles [cm^2/s]
D_F particles diffusivity (axial dispersion) in fluidized bed [cm^2/s, or m^2/h]
D_S inter-zone particles transfer [kg/h]
F_G gas flow rate [cm^3/s, or m^3/h]
F_j cross-section area in j-th zone [m^2]
h tortuosity of porous structure
h_q interphase heat-transfer coefficient [$kJ/(m^2\ h\ K)$]
h_R „radiator-to-bed“ heat-transfer coefficient [$kJ/(m^2\ h\ K)$]
H Henry coefficient [cm^3/g]
G_S flow rate of dry particles [kg/h]
G_{LPS}, G_{MPS} flow rate of water steam [kg/h]
k_m external mass-transfer coefficient [$cm^3/(cm^2\ s)$]
k_B, k_P local mass-transfer coefficient in bubble and particle [$cm^3/(cm^2\ s)$]
L_j height of j-th zone in bed [m]
L_c distance between pipes in radiator [cm]
R_P particles radius [cm]
R_m rate of mass transfer [g/s, or kg/h]
R_R rate of „radiator-to-bed“ heat-transfer [kJ/h]
R_q rate of interphase heat transfer [kJ/h]
r coordinate inside particle [cm]
Q_H, Q_W heat of vaporization of heptane and water [kJ/kg]
s particle shape parameter (0 – plate, 1 – cylinder, 2 – sphere)
S_B, S_P external surface of bubble and particle [cm^2 or m^2]
T_G, T_S, T_R temperature of gas bed and radiator [°C]
T_{LPS}, T_{MPS} temperature of water steam [°C]
u_G gas velocity [cm/s, or m/s]
u_F minimum fluidization velocity [cm/s, or m/s]
V_j volume of j-th zone [cm^3, or m^3]
V_B, V_P volume of bubble and particle [cm^3]
W, W_E current and equilibrium moisture of particles [g/g or kg/kg]
w dimensionless moisture Eq. (7))

Greek symbols

$\alpha_R = h_R a_R$ total „radiator-to-bed“ heat-transfer coefficient [$kJ/(m^3\ h\ K)$]
$\alpha_T = h_q\ a_B$ total interphase heat-transfer coefficient [$kJ/(m^2\ h\ K)$]
β_T total interphase mass-transfer coefficient [1/s or 1/h]
β_B, β_P total mass-transfer coefficient in bubbles and particles [1/h]
ε_P porosity of particles
ε_S, ε_F void fraction of a fixed and fluidized bed
ψ empirical parameter (Eq. (5))
$\phi = r/R_P$ dimensionless radius of particles
ρ_P polymer particles density [g/cm^3 or kg/m^3]
ρ_S, ρ_F density of fixed and fluidized bed [g/cm^3 or kg/m^3]
ρ_G, ρ_L density of gas and liquid [g/cm^3 or kg/m^3]
μ_G, μ_L viscosity of gas and liquid [g/(cm s)]
λ_G, λ_L heat conductivity of gas and liquid [J/(cm s K)]
λ_F heat conductivity of fluidized bed [kJ/(m h K)]
λ_S inter-zone heat transfer [kJ/(h K)]
τ_Z residence time of particles in bed [min or h]

Aknowledgments

The author would like to acknowledge G. Mijatović and B. Dimić for survey work on the trial run of dryer.

REFERENCES

[1] A.V. Lykov, Theory of energy and mass transfer, Prentice-Hall, Englewood Cliffs, NJ, 1961.
[2] D. Kunii, O. Levenspiel, Fluidization Engineering, 2nd ed. Butterworth-Heinemann, Boston, MA, 1991.
[3] A.V. Lykov, Heat and mass transfer (Handbook), Energia, Moscow, 1972 (in Russian).
[4] R.C. Reid, J.M. Prausnitz, T.K. Sherwood, The properties of gases and liquids, McGraw-Hill, New York, 1977.
[5] J.A. Debling, W.H. Ray, Heat and mass transfer effects in multistage polymerization processes, Ind. Eng. Chem. Research **34** (1995) 3466–3480.
[6] Perry’s Chemical Engineers’ Handbook, McGraw-Hill, New York, 1984.
[7] Fluidization, J.F. Davidson, D. Harrison, Eds., Academic Press, London, 1971.
[8] M. Schreiber, T.W. Asegehegn, H.J. Krautz, Numerical and Experimental Investigation of Bubbling Gas- Solid Fluidized Beds with Dense Immersed Tube Bundles, Ind. Eng. Chem. Research **50** (2011) 7653–7666.
[9] M. Rudisuli, T.J. Schildhauer, S.M.A. Biollaz, J.R. van Ommen, Radial Bubble Distribution in a Fluidized Bed with Vertical Tubes, Ind. Eng. Chem. Research **51** (2012) 13815–13824.
[10] S. Sanaei, N. Mostoufi, R. Radmanesh, R. Sotudeh-Gharebagh, C. Guy, J. Chaouki, Hydrodynamic Characteristics of Gas- Solid Fluidization at High Temperature, Canadian J. Chem. Eng. **88** (2010) 1–11.

IZVOD

SUŠENJE POLIMERNOG PRAHA U FLUIDIZOVANOM SLOJU. MODELIRANJE VIŠESLOJNE SUŠNICE

Nikolaj M. Ostrovski

Hipol a.d., Odžaci, Serbia

(Naučni rad)

Analiziran je proces sušenja poroznih čestica polimera (polipropilena) sa ciljem uklanjanja rastvarača (heptana). Sušnica uključuje dva stadijuma (aparata) sa fluidizovanim slojem u kojima postoje nekoliko zona sušenja. Predložen je matematički model procesa u fluidizovanom sloju sa različitim zonama. Određen je limitirajući stupanj sušenja u zavisnosti od prečnika polimernih čestica. Pronađeno je da u relativno krupnim česticama (>200 μm) brzina sušenja se limitira difuzijom unutar čestica. U malim česticama (<50 μm) proces limitira prenos mase kroz spoljašnu površinu mehuriča gasnog fluida (azota). Model je pokazao zadovoljavajuću saglasnost sa eksperimentalnim podacima i korišćen je za optimizaciju rada sušnice. Data je analiza načina smanjenja potrošnje energije koje su ispitane u eksperimentima na industrijskom postrojenju.

Ključne reči: Sušenje polimernog praha • Fluidizovani sloj • Limitirajući stupanj • Zone sušenja • Matematički model